FEBS Letters 589 (2015) 476–483

journal homepage: www.FEBSLetters.org

Respiratory complexes III and IV can each bind two molecules of cytochrome *c* at low ionic strength

Blas Moreno-Beltrán [a], Irene Díaz-Moreno [a,*], Katiuska González-Arzola [a], Alejandra Guerra-Castellano [a], Adrián Velázquez-Campoy [b,c,d], Miguel A. De la Rosa [a], Antonio Díaz-Quintana [a]

[a] Instituto de Bioquímica Vegetal y Fotosíntesis, cicCartuja, Universidad de Sevilla-CSIC, Avda. Américo Vespucio 49, Sevilla 41092, Spain
[b] Institute of Biocomputation and Physics of Complex Systems (BIFI) – Joint Unit BIFI-IQFR (CSIC), Universidad de Zaragoza, Mariano Esquillor s/n, 50018 Zaragoza, Spain
[c] Departamento de Bioquímica y Biología Molecular y Celular, Universidad de Zaragoza, Pedro Cerbuna 12, 50009 Zaragoza, Spain
[d] Fundacion ARAID, Government of Aragon, Maria de Luna 11, 50018 Zaragoza, Spain

ARTICLE INFO

Article history:
Received 6 November 2014
Revised 26 December 2014
Accepted 7 January 2015
Available online 14 January 2015

Edited by Peter Brzezinski

Keywords:
Cytochrome *c*
Cytochrome bc_1
Cytochrome *c* oxidase
Isothermal Titration Calorimetry
Nuclear Magnetic Resonance
Supercomplex

ABSTRACT

The transient interactions of respiratory cytochrome *c* with complexes III and IV is herein investigated by using heterologous proteins, namely human cytochrome *c*, the soluble domain of plant cytochrome c_1 and bovine cytochrome *c* oxidase. The binding molecular mechanisms of the resulting cross-complexes have been analyzed by Nuclear Magnetic Resonance and Isothermal Titration Calorimetry. Our data reveal that the two cytochrome *c*-involving adducts possess a 2:1 stoichiometry – that is, two cytochrome *c* molecules per adduct – at low ionic strength. We conclude that such extra binding sites at the surfaces of complexes III and IV can facilitate the turnover and sliding of cytochrome *c* molecules and, therefore, the electron transfer within respiratory supercomplexes.

1. Introduction

Cytochrome c_1 (Cc_1) is the subunit of mitochondrial complex III (III), or cytochrome bc_1 (Cbc_1), responsible for electron transfer (ET) to cytochrome *c* (C*c*) and, in turn, to complex IV (IV), or cytochrome *c* oxidase (C*c*O) [1–5]. This function is essential for mitochondrial respiration, the major source of energy in eukaryotic cells. The organization of the mitochondrial electron transport chain is a subject of intense debate at present, where two different models are being considered: the fluid model, that proposes a random organization for individual respiratory protein components, and the solid model, suggesting a stable association between individual complexes [6–8]. Apart their role in respiration, C*c* and Cc_1 are clearly involved in the development of programmed cell death [9–15]. Such a dual role of C*c* is regulated by post-translational modifications – namely, phosphorylation and nitration of tyrosine residues – that affect the binding of C*c* to its physiological counterparts, either in the mitochondria or in the cytoplasm [16–23].

The ET reactions between C*c* and its partners Cbc_1 and C*c*O have been characterized by time-resolved spectroscopy and steady-state enzyme kinetic studies [24–28]. Both, reduction and oxidation of C*c* show multiphasic kinetic traces in polarographic and spectrophotometric studies. This suggests the presence of at least two binding sites in the C*c* partners: a catalytic ET site, along with an adjacent, non-productive site. In agreement with this, we have recently reported that plant C*c* (pC*c*) docks at two binding sites of plant Cc_1 (pCc_1) [29]: The first, *proximal* site is suitable for ET between both hemeproteins and resembles that previously determined by X-ray diffraction in yeasts [30]; the second, *distal* site localizes close to the Rieske subunit and seems to be involved in channeling of C*c* molecules toward C*c*O [29,31,32]. Classical

Abbreviations: CSP, Chemical-Shift Perturbations; Cbc_1, cytochrome bc_1; C*c*, cytochrome *c*; C*c*O, cytochrome *c* oxidase; Cc_1, cytochrome c_1; (III), complex III; (IV), complex IV; DLS, dynamic light scattering; ET, electron transfer; K_D, equilibrium dissociation constant; HSQC, Heteronuclear Single-Quantum Correlation; hC*c*, human cytochrome *c*; hC*c*1, human cytochrome c_1; IMS, intermembrane mitochondrial space; IMM, inner mitochondrial membrane; ITC, Isothermal Titration Calorimetry; LB, Luria-Bertani; MM, mitochondrial matrix; NMR, Nuclear Magnetic Resonance; pC*c*, plant cytochrome *c*; pC*c*1, plant cytochrome c_1; PCA, Principal Component Analysis; C*c*O$_{red}$, reduced cytochrome *c* oxidase; hCc_{red}, reduced human cytochrome *c*; pCc_{1red}, reduced plant cytochrome c_1

* Corresponding author. Fax: +34 954460165.
E-mail address: idiazmoreno@us.es (I. Díaz-Moreno).

http://dx.doi.org/10.1016/j.febslet.2015.01.004

crosslinking assays between C*c* and C*bc*$_1$ had already pointed out that residues from the *distal* site of C*c*$_1$ could be involved in the interaction with C*c* [33].

The study of heterologous complexes, also known as cross-complexes, is a widely accepted approach to get insight into the binding mode of interprotein complexes [34,35]. To provide further insight into the nature of the interactions between C*c* and C*c*$_1$, we analyze here the cross-complex between human C*c* (hC*c*) and pC*c*$_1$, and compare it with the natural pC*c*–pC*c*$_1$ complex in plants in terms of binding affinity, specificity and dynamics. Actually, the turnover number for reduction of mammalian C*c* by potato C*bc*$_1$ is similar than that for the mammalian C*c*–C*bc*$_1$ system [28]. As there are substantial differences in the electrostatic potential surface of pC*c* and hC*c*, the analysis of the hC*c*–pC*c*$_1$ complex is a very useful approach to better understand the C*c*–C*c*$_1$ binding mode. In fact, the major differences between the two C*c* orthologs are at their respective surfaces in contact with pC*c*$_1$ (Fig. 1). Given the relevance of electrostatics in C*c*–C*c*$_1$ complexes, the ionic-strength dependence of the binding event has also been addressed, so revealing a crucial role in both the binding affinity between the partners and the definition of the binding sites on the pC*c*$_1$ surface. In addition, the hC*c*–pC*c*$_1$ interaction has been compared with that between hC*c* and bovine C*c*O. Notably, C*c* also interacts with two binding sites on C*c*O. Altogether, our data provide a better comprehension of the molecular recognition processes involved in mitochondrial respiration.

2. Material and methods

2.1. Modelling

pC*c* and pC*c*$_1$ models were built in previous work [29]. hC*c* structure was taken from Protein Data Bank (PDB ID: 3zcf) [36]. Human cytochrome *c*$_1$ (hC*c*$_1$) model was built following the same procedure reported for pC*c*$_1$ model [29]. The electrostatic potential surfaces of pC*c*, pC*c*$_1$, hC*c*, and hC*c*$_1$ structures were calculated using DelPhi [37] and Chimera [38]. The electrostatic potential surfaces were calculated assuming an ionic strength of 250 mM.

2.2. Protein expression and purification

Escherichia coli BL21 (DE3) cells transformed with pBTR1 plasmid were used to produce recombinant hC*c* [39]. ^{15}N-labeled hC*c* was expressed in M9 minimal medium for Nuclear Magnetic Resonance (NMR) titrations, whereas unlabeled hC*c* was produced in Luria-Bertani (LB) medium for Isothermal Titration Calorimetry (ITC) measurements. Expression and purification protocol was similar to that recently described for pC*c* [29], excepting the cell culture was at 30 °C and the elution gradient for the cationic exchange column, which ranged from 0.036 to 0.36 M NaCl. The optimization of the expression and purification steps was carried out according to specific protocols for *c*-type cytochromes [40–43]. The yield of hC*c* was 15-20 mg/L in LB and 10–15 mg/L in M9 minimal medium.

Unlabeled pC*c*$_1$ was expressed and purified as described previously [29]. Bovine C*c*O was purchased from Sigma and used after exchanging its buffer in Millipore 3 K NMWL centricons to 10 mM sodium phosphate buffer (pH 7.4) containing 0.2% n-Dodecyl-β-D-maltoside and 5 mM sodium dithionite. The pH of the buffer was checked before and after the sample preparation. Fresh samples were used to carry out the experiments. Dynamic Light Scattering (DLS) assays were performed to evaluate the oligomerization state of the C*c*O at the protein concentration used in ITC titrations, in which C*c*O was predominantly monomeric (75%). DLS experiments were conducted at 25 °C in a Zetasizer Nano ZS (Malvern).

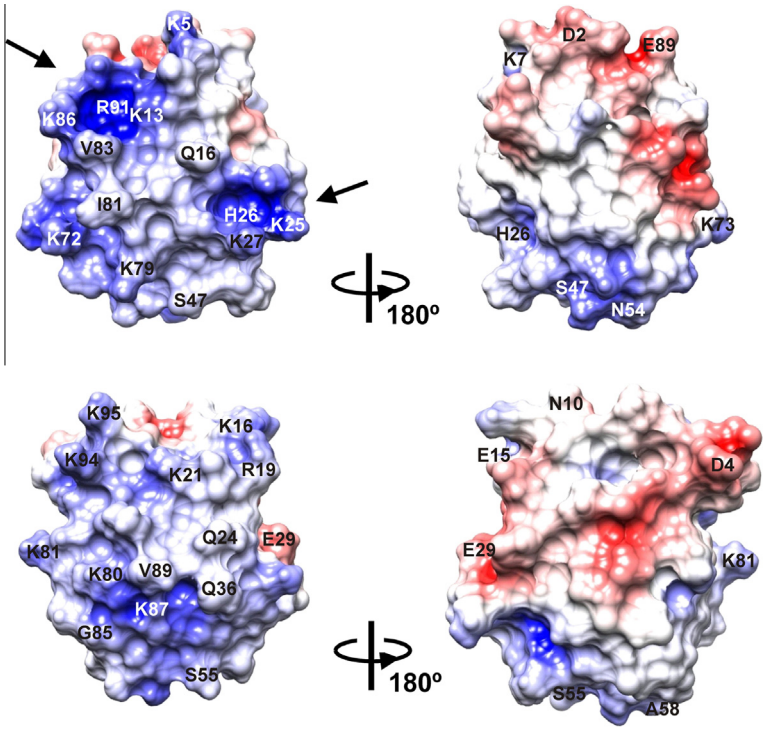

Fig. 1. Electrostatic surface potential of hC*c* and pC*c*. Negatively and positively charged regions of hC*c* (*upper*) and pC*c* (*lower*) surfaces are depicted in red and blue colors, respectively. The color scale ranges from −5 (red) to +5 (blue) k_BT. Some residue numbers have been mapped to better show the orientation of hC*c* and pC*c* in the figure. The arrows highlight two electropositive regions at the hC*c* surface. The simulation was performed using DelPhi aided by Chimera, assuming an ionic strength of 250 mM. The interior and exterior dielectric constants were fixed to 2 and 80, respectively.